This is the accept manuscript of the following article that appeared in final form in Microporous and Mesoporous Materials 250: 88-99 (2017), which has been published in final form at https://doi.org/10.1016/j.micromeso.2017.05.020.

Upgrading of sewage sludge by demineralization and physical activation with CO_2: application for methylene blue and phenol removal

Irene Sierra[1*], Unai Iriarte-Velasco[1], Mónica Gamero[2] and Andrés T. Aguayo[2]
[1]Department of Chemical Engineering, Faculty of Pharmacy, University of the Basque Country (UPV/EHU), Vitoria-Gasteiz, Spain.
[2]Department of Chemical Engineering, Faculty of Science and Technology, University of the Basque Country (UPV/EHU), Leioa, Spain.
*Corresponding author. Tel.: +34 945013290; fax: +34 945013014. E-mail:

irene.sierra@ehu.eus

Abstract

Carbon-based adsorbents were prepared by the physical activation of sewage sludge with CO_2 through an integrated method (without a precarbonization stage). The activation was conducted at different temperatures (600-1000 ºC), and the effect of the acid washing, performed either before or after the physical activation, was investigated. From the standpoint of textural properties, the optimum activation temperature is between 800-900 ºC; higher temperatures cause an important reduction in porosity. The acid post-washing significantly increases the porosity in the whole pore size range due to the removal of the inorganic fraction and pore unblocking. Both the activation temperature and the acid treatment strongly affect the surface chemistry. The uptake of methylene blue correlates significantly with textural properties (such as BET surface area), but also with surface chemistry (carbonyl groups). The combination of a moderate activation temperature (600 ºC) and acid post-washing results in a cost-effective material with a suitable methylene blue removal ability. On the contrary, the adsorption of phenol, favoured by materials with a high degree of microporosity, is maximized by acid pretreatment prior to activation at 900 ºC.

Keywords: Sewage sludge; carbon dioxide; acid washing; phenol; methylene blue.

1. Introduction

The amount of sewage sludge has rapidly increased in the last decades, as a consequence of the urbanization and industrial development. The traditional methods to utilize or dispose sewage sludge are land filling, incineration and composting for farmland application [1]. However, these disposal routes are limited, due to more stringent environmental standards, and increasing costs. Thus, the development of environmentally friendly solutions is of main interest. Among them, the conversion of sewage sludge into carbon-based adsorbents is a promising alternative [2,3]. Indeed, apart from being an eco-friendly alternative to solve the problem of secondary pollution, it also allows its reuse in water treatment.

This valorization procedure commonly includes the chemical activation with different reagents such as H_2SO_4 [2-4], H_3PO_4 [5-7], KOH [6,8-10], NaOH [9,11], $ZnCl_2$ [5,10,12] and K_2CO_3 [6,10,13]. Carbon-rich sewage sludge can be also physically activated, using gasifying agents such as steam [14,15], air [16,17] and CO_2 [18-20]. Usually, sewage sludge is carbonized prior to the activation process at relatively low temperature (400-700 ºC) to break down the cross-linkage between carbon atoms, thus allowing a greater impact of the subsequent activation step [21]. During the physical activation of sludge carbon (SC) pores can be formed through several processes: (i) the loss of water and the decomposition of organic matter [1,22]; (ii) the thermal decomposition of inorganic compounds, such as salts, which are released as gaseous products [16] and (iii) the progressive burn-off of the carbon fraction by the gasifying agent, which is effective to develop the micropore structure of the material [23].

The development of porosity in a sewage sludge-derived material is limited by the high inorganic content of the precursor, which is essentially non-porous. It has been reported that the acid washing of sludge can remove part of its mineral content, responsible for pore blockage

upon calcination, resulting in a significant increase of porosity [11,20,22]. The acid washing prior to physical activation has been reported to be effective [11], since: (i) it reduces the conversion of the inorganic fraction into mineral-like compounds, and the encapsulation of some metals by the carbon phase [24], phenomenon which takes place at high temperature; (ii) sewage sludge is subjected to a combined physical and chemical activation process. However, recent studies revealed that the excessive removal of minerals before the activation step can eliminate the catalytic activity of minerals during the thermal treatment [25,26]. The optimum acid washing sequence remains unclear, as there is no comprehensive study in the literature comparing the effect of pre- and post-washing.

This paper approaches the preparation of adsorbents based on sewage sludge, through physical activation with CO_2. This agent was selected because it has been less studied than steam. Moreover, the sequestration and valorization of CO_2 is an issue of great concern. The activation process was performed through an integrated method, without a precarbonization stage. This preparation protocol results in a considerable reduction of the preparation cost, due to energy saving and the higher carbon yield attained [27]. The study was conducted in a wide range of activation temperature (600-1000 ºC) to determine whether the reaction of CO_2 with carbon is favoured. Furthermore, the effect of the acid treatment (either before or after physical activation) was investigated, in order to seek synergies between the activation with CO_2 and the acid treatment. Special attention was paid to the investigation of the porous structure of the materials, since a recent review pointed out the lack of sufficient information about the pore size distribution [27]. A preliminary study of the activation mechanism was also made, using thermogravimetric analysis coupled to mass spectrometry. Finally, the adsorption performance of the materials was studied for two aqueous pollutants: methylene blue and phenol.

2. Experimental

2.1. Raw material

Anaerobically digested and dewatered sewage sludge was collected from an urban wastewater plant. Raw sludge was dried in a convection oven at 105 ºC for 48 h to achieve a constant weight. Table 1 shows the proximate analysis of raw sludge. It is characterized by a high moisture content (73.3 wt%), whereas the percentage of fixed carbon is relatively low (8.6 wt%). Dried sludge has a similar content of volatile matter and ash (49.2 and 42.2 wt%, respectively).

Table 1. Proximate analysis of raw dewatered sewage sludge (wt%). Results are expressed on a dry basis, except for water content.

Constituents	Moisture	Volatile matter	Fixed carbon	Ash
Value	73.3	49.2	8.6	42.2

Dried sludge was analysed by thermogravimetry (TG) using a SDT 2960 thermobalance (T.A. Instruments). The analysis was performed under both inert (nitrogen) and oxidant (air) atmospheres. About 15-20 mg of sample were put into the alumina crucible and heated from room temperature to 800 ºC, at a heating rate of 10 ºC/min. In order to detect the compounds released during the thermal analysis, exhaust gases were analysed on-line by mass spectrometry (MS), using a Balzers Instruments EM Thermostar equipment.

2.2. Preparation of sludge carbon

Dried sludge was grinded and sieved, and particles within the 0.5-1.0 mm range were selected. Three preparation protocols were investigated: first, by applying only physical activation, second; by applying the acid treatment before thermal activation (thereafter referred as acid pretreated) and third; by applying acid treatment after thermal activation (thereafter referred as

acid washed). Acid-pretreated samples were not rinsed with water before thermal activation. Consequently, those samples were subjected to a combined physical and chemical activation process.

Physical activation was conducted as follows: sample was introduced in a quartz tube furnace under CO_2 flow (120 cm^3/min, corresponding to 8 minutes of residence time), Temperature was increased from room temperature to 600-1000 ºC at a rate of 15 ºC/min. Samples were soaked at the final temperature for 30 min, and then cooled down in a N_2 atmosphere.

The acid treatment was carried out as follows: about 1 g of sample was contacted with 20 cm^3 of HCl (3 M) solution. Solutions were introduced in 50 ml borosilicate amber glass vials and stirred at 120 rpm in a reciprocating shaker at room temperature for 48 h, to ensure the access of the acid to the interior of the particles. Finally, samples were filtered, transferred to a convection oven and dried at 80 ºC for 24 h.

Samples of sludge carbon (SC) prepared only by physical activation with CO_2 were coded according to the activation temperature: SC-600, SC-700, SC-800, SC-900 and SC-1000. Samples of acid-washed SC were coded indicating the activation temperature, and acid washing sequence, either prior to (P) or after (A) physical activation: PSC-600, PSC-700, PSC-800, PSC-900 and PSC-1000, SCA-600, SCA-700, SCA-800, SCA-900 and SCA-1000. Before adsorption tests, all samples were extensively washed in fixed bed with 600 bed volumes of distilled water, until a constant pH was obtained.

2.3. Characterization of sludge carbon

The textural properties of the prepared materials were determined by nitrogen adsorption/desorption (Micromeritics ASAP 2010). The specific surface area was determined by the Brunauer-Emmett-Teller (BET) method. The micropore surface area and volume were

obtained using the t-plot method, whereas mesopore and macropore values were determined based on the Barrett, Joyner & Halenda (BJH) method.

The acidity/basicity of samples of sludge carbon was measured as described by Tessmer et al. [28]. The ash content was measured by heating the samples at 815 ºC under air atmosphere for 1 h (UNE 32004 standard).

Elemental analysis was performed using CHNS analyzer (EuroVector EA-3000, Italy). The total concentration of heavy metals (Cr, Ni, Cu, Zn and Pd) in sludge carbons was determined by a high performance Inductively Coupled Plasma Mass Spectrometer (ICP-MS, 7500ce Agilent Technologies). Prior to heavy metal determination, the sludge samples were microwave digested (Speedwave Four, Berghof) using an acid mixture (HNO_3:HF = 3:1).

Fourier transform infrared (FTIR) measurements were performed using a Thermo Nicolet 6700 device in the absorbance mode, using the KBr self-supported pellet technique. Spectra were collected in the 400-4000 cm^{-1} range with a resolution of 2 cm^{-1}.

2.4. Adsorption experiments

Methylene blue (MB) and phenol were selected as target adsorbates based on their different molecular size and physicochemical properties. MB is a basic dye and has been used as an indicator of the nature and amount of the adsorption sites in the micropore and mesopore range. Phenol is an acid compound, and due to its smaller molecular size it has been used as an indicator of adsorption capacity in the micropore range.

In the adsorption experiments, about 10-15 mg of SC were contacted in stoppered glass bottles with 10 cm^3 of aqueous solutions of MB (in the 25-100 mg/L range) or phenol (in the 25-250 mg/L range). The flasks containing the suspension were shaken for 72 h using a rotary mixer

placed in a thermostatic chamber at 20 ºC ± 0.5 ºC. Preliminary adsorption experiments showed that a holding time of 72 h was enough for the suspension to reach the equilibrium. After 72 h, samples were centrifuged and the residual concentration of the solute in the supernatant was analysed by means of a UV/VIS spectrophotometer (Jasco V-630). The concentration of MB and phenol was determined by recording the UV absorbance at a wavelength of 662 nm and 270 nm, respectively. The spectrophotometer was previously calibrated using standard solutions of methylene blue and phenol.

The adsorption capacity of samples of sludge carbon (q_e, mg/g) was calculated by mass balance:

$$q_e = (C_0 - C_e) \cdot V/m \quad (1)$$

where C_o and C_e are the initial and equilibrium concentrations of the adsorbate (mg/L), respectively. V is the solution volume (L) and m the adsorbent mass (g).
Randomly selected experiments were carried out in triplicate, and the mean values were reported.

The adsorption isotherms of both adsorbates (MB and phenol) were determined. The equilibrium data were fitted to the well known Langmuir, Freundlich and Redlich-Peterson (Eq. 2) equations:

$$q_e = \frac{K_R \cdot C_e}{1 + \alpha \cdot C_e^{\beta}} \quad (2)$$

where K_R is the Redlich-Peterson constant (L/g), α is a constant having units of $(L/mg)^{\beta}$, and β is an exponent that lies between 0 and 1.

The parameters of best fit were calculated by non-linear regression. The goodness of fit between the experimental and calculated values was determined by means of the average percentage error (APE):

$$APE = \frac{\sum_{i=1}^{n} \left| \left(q_{e,exp} - q_{e,pred} \right) / q_{e.exp} \right|}{n} \cdot 100 \quad (3)$$

where $q_{e,exp}$ is the experimentally measured uptake capacity, $q_{e,pred}$ is the predicted uptake capacity and n the number of experiments.

3. Results and discussion

3.1. Characterization of raw sludge

Figure 1 displays the TG and DTG results of raw sludge under nitrogen and air atmospheres. The combustion curve of raw sludge is under the pyrolysis curve throughout all the run, as a result, the total loss of mass is higher for the combustion run (57.8 vs. 49.1 wt%). At mild temperatures (below 350 ºC) the difference between both weight-loss curves is around 5 % which increases to around 14 percentage points at higher temperatures. The fact that the combustion curve does not show a strong decay at high temperatures reveals that it corresponds to oxidative pyrolysis or accelerated pyrolysis, in which oxygen accelerates the decomposition rate compared to the pyrolysis, and the char formed is burnt simultaneously to its formation. The oxidative pyrolysis is characteristic of the type of raw material used in this work, anaerobically digested sewage sludge, as reported by Font et al. [29].

FIGURE 1

The thermal behaviour of raw sludge under an oxidizing atmosphere provides information about the organic matter composition and its degree of polymerization. According to the data reported by Gascó et al. [30], the small weight loss observed at low temperature (21 wt% at 300 ºC) reflects a well-stabilized sewage sludge. The low mass loss at high temperature (above 600 ºC) is indicative of a low degree of polymerization and aromatization [30,31].

In both oxidative and inert atmospheres, the weight loss takes place through different stages. The first step (below 150 ºC) is ascribed to the evaporation of adsorbed water. The main stage of weight loss occurs at intermediate temperatures (175-500 ºC). In the derivative mass loss curve of the pyrolysis run two overlapping peaks can be observed at this temperature range with maxima at 290 and 330 ºC, as well as a shoulder peak near 440 ºC. A similar profile was reported by others [32,33]. The mass loss in this temperature interval is more pronounced under oxidative conditions, revealing a stronger desorption of constitution water and decomposition and volatilization of organic matter, in addition to the oxidation of organic matter [15,34]. The last step of mass loss occurs at temperatures above 600 ºC, and is commonly attributed to the thermal decomposition of calcium carbonate and sulphate.

FIGURE 2

Figure 2 shows the mass spectrometric curves of the main compounds released during the thermal treatment of raw sludge under inert and oxidizing atmosphere. High amounts of water are released under both combustion and pyrolysis conditions. It is noteworthy that water is released in the whole temperature range in good agreement with the results reported by Conesa et al. [35]. The first peak, below 175 ºC, is attributed to the release of capillary and adsorbed water. At higher temperatures, the release of water is ascribed to constitution water [15] or to its formation through different reactions. Under oxidative conditions, the combustion of hydrogen-containing compounds results in better defined water release peaks in the 200-500 ºC range.

Carbon dioxide was detected in both experiments, including the pyrolysis, in good agreement with the product distribution reported by others [33,35]. The release of CO_2 occurs in the 200-500 ºC range and above 550 ºC irrespective of the atmosphere. The release in the 200-500 ºC range occurs in two steps and is partially ascribed to the above-mentioned decomposition and

volatilization of organic matter [36]. Moreover, in the case of the oxidizing atmosphere, the combustion of carbonaceous materials leads to a higher release of CO_2. The CO_2 detected above 600 ºC is ascribed to decomposition of calcium carbonate and sulphate [15,22,37]. It is noteworthy that in the pyrolysis run, a similar release of CO_2 takes place both above 600 ºC and in the 200-500 ºC range whereas in the oxidation run, the CO_2 release in the low temperature range is significantly higher.

NO was detected only under oxidizing conditions (Figure 2b). It occurs in the 200-500 ºC temperature range, and takes place in two steps. Its absence in the pyrolysed sample suggests that it is formed through the combustion of nitrogen-containing compounds.

Cyanides are released in the 200-500 ºC temperature range. Several authors have also detected CN^- during the activation of different carbonaceous precursors [34,35,38]. Robau-Sánchez et al. [38] reported the release of CN^- during the alkaline activation with KOH of *Quercus agrifolia* char, and developed different reaction mechanisms that lead to the formation of cyanides in both liquid and gas form. According to these reaction mechanisms, the essential conditions to form cyanides are the presence of OH^- functionalities, and a source of carbon and nitrogen. Regarding sewage sludge, OH^- groups have been identified by FTIR. Moreover, it is expected that both structural carbon and nitrogen take part in the generation of cyanides.

Methane was detected in effluent gases as shown in Figure 2, which is in good agreement with the product distribution reported in the literature for the pyrolysis of sewage sludge under helium [39], nitrogen [35] and argon atmosphere [33]. The presence of CH_4 under oxidizing conditions reveals that part of the methane formed during the thermal treatment remains unburned. Methane is released in two steps, with their maxima near 300 ºC and 450 ºC. Its formation should be partially attributed to the above-mentioned reactions of cyanide formation [38], which imply the simultaneous formation of methane. However, the difference in the shape

of both curves (methane and cyanides) suggests the existence of additional processes of methane release, such as the thermal decomposition of organic matter.

3.2. Sludge carbon yield and ash content

Table 2 summarizes the values of ash content, and partial and overall yields for the prepared samples of sludge carbon. The physical activation yield (Y_{phys}, on a dry basis) was obtained using the weight of the sample before and after the physical activation with CO_2. The yield of the acid treatment (Y_{acid}) was calculated as the ratio between the mass of the sample after and before the treatment with HCl. The overall yield of sludge carbon (Y_{SC}) was calculated as the product of the individual yields.

As expected, the physical activation yield decreases with temperature, whereas the ash content increases. These results are associated with the concentration of non-mineral constituents, and also to the devolatilization of solid hydrocarbons and the gasification of carbonaceous residues at high temperature. It is noteworthy that the physical activation yield is lower for the samples pretreated with HCl (PSC). This suggests that the hydrochloric acid takes part in the activation mechanism, by combination of physical and chemical activation. Regarding the chemical yield (Y_{acid}), it is about 66% for the pretreated samples (PSC) whereas it decreases to about 50% for the acid washed samples (SCA).

Table 2. Overall carbon yield and partial yields of different preparation steps (physical activation and acid washing), ash content and pH.

Sample	Y_{phys} (wt%)	Y_{acid} (wt%)	Y_{SC} (wt%)	Ash content (wt%)	pH
SC-600	60.5	-	60.5	64.4	11.1
SC-700	57.7	-	57.7	67.3	11.3
SC-800	52.1	-	52.1	76.2	11.3

SC-900	42.2	-	42.2	92.2	11.3
SC-1000	38.7	-	38.7	99.8	11.4
SCA-600	60.5	50.4	30.5	38.6	5.2
SCA-700	57.7	49.3	28.4	41.0	5.3
SCA-800	52.1	45.1	23.5	49.8	5.4
SCA-900	42.2	47.8	20.2	72.7	5.8
SCA-1000	38.7	44.3	17.1	-	-
PSC-600	53.1	66.3	35.2	53.4	3.5
PSC-700	50.9	66.3	33.8	56.0	4.0
PSC-800	46.0	66.3	30.5	60.0	5.5
PSC-900	36.4	66.3	24.2	77.7	6.8
PSC-1000	29.3	66.3	19.4	99.6	7.3

3.3. Characterization of sludge carbon

3.3.1. Textural properties

Figures 3 shows the pore size distribution (PSD) of the prepared samples of sludge carbon, measured by the BJH method (dV vs d_p is given as supplementary material in Figure S1). It is observed that the materials have a hierarchical porous structure, and a highly mesoporous and macroporous nature. Table 3 summarizes the values of the textural properties.

For samples prepared by physical activation only, the highest value of S_{BET} (113 m^2/g) and total pore volume (0.156 cm^3/g) is obtained using an activation temperature of 800 ºC. The optimum value of micro- (S_{micro} of 40.7 m^2/g) is also obtained for SC-800. Lower temperatures are inefficient to develop porosity, whereas higher temperatures results in a decrease of porosity. In fact, a temperature of 1000 ºC leads to an important destruction of the porosity (Figure 3a, Table 3) associated with pore deformation, cracking or blockage phenomena [40]. It is noteworthy that, in SC-800 sample, the main contribution to specific surface area arises from pores smaller

than 80 Å. The effect of activation temperature is especially strong at this pore range (Figure 3a).

FIGURE 3

The acid washing with HCl after physical activation causes a significant increase in the porosity (Figure 3, Table 3). The maximum value of S_{BET} (339 m^2/g) and total pore volume (0.486 cm^3/g) in this series was observed for sample activated at 800 ºC. It also exhibits the highest value of S_{micro}, V_{micro} and V_{meso}. Data regarding activation at 1000 ºC are not presented since the acid washing resulted in a too small particle size, below that used in this study. Nevertheless, based on the properties of SC-1000, good textural properties could not be expected.

The analysis of the pore size distribution of SCA samples (Figure 3b) gives some insight into the pore development and unblocking process. The contribution of small mesopores (dp < 80 Å) is maximum for the sample activated at 700 ºC (i.e. SCA-700 is the upper curve in both specific surface area and pore volume). On the contrary, SCA-800 exhibits the highest amount of large mesopores (80-500 Å range). These results suggest that higher temperatures result in the formation of larger pores up to 800 ºC. A further increase in temperature leads to an important decrease in porosity.

The comparison of the data of SC (Fig. 3a) and SCA series (Fig. 3b) reveals an outstanding increase in the specific pore area after the washing step. The values of S_{BET} of SCA samples are about two to three fold larger than the largest value in the SC series. This increase is observed in the whole pore size range (i.e. at 600 ºC, pore area in the micro-, meso- and macropore range increases by 367, 204 and 105%, respectively). This effect is visible for all the activation temperatures studied. According to data in Table 3, micropores, formed to a great extent due to the burn-off of carbon with CO_2 [23], remain hidden due to pore blockage. The acid washing

step removes part of the inorganic fraction that blocks the porous structure and textural properties become visible, resulting in a better accessibility to pores. Our results reveal that washing with HCl is advisable when physical activation is performed with CO_2.

The corrected BET value, as given by Equation (4) [11], was used to ascertain whether the increase in porosity is due only to the removal of inorganic matter (which is essentially non porous). This value assumes that the inorganic matter does not contribute to the specific surface area:

$$\text{Corrected } S_{BET} = \frac{\text{measured } S_{BET}}{1 - \text{ash content (mass fraction)}} \quad (4)$$

The corrected BET values are represented in Figure 4. The results corresponding to an activation temperature of 1000 ºC were not represented, since the amount of organic matter is very low.

FIGURE 4

The corrected BET values of acid washed samples (SCA) are still considerably higher than those of non treated samples (SC), which confirms that the improvement in the specific surface is due to alterations in the porous structure (such as pore unblocking) rather than only the removal of the inorganic fraction. Also, SC and SCA samples exhibit an increasing trend of corrected S_{BET} with temperature in the 600-900 ºC range.

The acid pretreatment has a detrimental effect in the specific surface area at activation temperatures lower than or equal to 800 ºC (Figure 3c). As a consequence of the acid pretreatment, thin pore walls in the raw material are destroyed. For example, at 600ºC, the S_{BET}

is reduced by two thirds as compared to SC samples, and macropore volume is maximum within that series (Table 3, V_{macro} = 0.0798 cm^3/g) as small micropores are merged.

The pretreatment only has a positive effect when the activation process is carried out in the 800-900 ºC range, as revealed by the highest values of S_{BET} in the PSC series (Table 3). The pretreatment leads to an enhancement of the micropore network, compared to SC samples. For example, S_{micro} is 3.5 m^2/g for SC-900 and 109 m^2/g for PSC-900. This result suggests that high activation temperatures are required in order for HCl to have an effect in the heating stage. The increase of porosity could be due to either specific reactions during the combined physical and chemical activation, or to the aforementioned pore unblocking.

Table 3. Textural properties of the prepared samples of sludge carbon. S m^2/g; V cm^3/g, D_p, Å

	S_{BET}	S_{micro}[a]	S_{meso}[b]	S_{macro}[b]	V_{micro}[a]	V_{meso}[b]	V_{macro}[b]	V_{total}[c]	D_p[d]
SC-600	58.4	15.0	34.3	2.1	0.0063	0.0885	0.0489	0.144	78.4
SC-700	50.7	11.5	30.8	3.9	0.0048	0.0825	0.0554	0.143	84.1
SC-800	113	40.7	44.0	0.8	0.0178	0.0923	0.0462	0.156	50.5
SC-900	43.1	3.5	29.9	2.5	0.0013	0.0693	0.0707	0.141	84.7
SC-1000	3.5	0.6	0.4	0.1	0.00006	0.0009	0.0021	0.003	28.9
SCA-600	260	70.1	104.2	4.3	0.0313	0.1907	0.1006	0.323	47.6
SCA-700	290	29.2	174.2	4.3	0.0147	0.2882	0.0979	0.401	56.1
SCA-800	339	122	149.2	5.5	0.0539	0.3255	0.1066	0.486	57.0
SCA-900	212	64.5	84.5	6.3	0.0281	0.1725	0.1451	0.346	52.3
PSC-600	20.9	10.2	7.7	2.9	0.0044	0.0227	0.0798	0.107	69.8
PSC-700	16.9	8.9	5.7	2.1	0.0038	0.0173	0.0538	0.075	68.3
PSC-800	142	112	14.1	0.9	0.0485	0.0286	0.0220	0.099	26.0
PSC-900	164	109	32.6	1.9	0.0474	0.0758	0.0442	0.167	37.0
PSC-1000	16.3	8.0	2.7	1.0	0.0033	0.0054	0.0254	0.034	34.9

[a]t-plot method

[b]BJH method (adsorption branch)

[c]Sum of t-plot and BJH methods

[d]BET method

In any case, the maximum values of total specific surface area and pore volume are still well below those obtained by post washing, and the corrected S_{BET} of PSC-900, though very similar, is still inferior to SCA-900. The acid washing, performed once the porous structure has been developed, ensures a better accessibility of the activating agent to the interior of the particles, resulting in a better removal of the inorganic fraction. The data of ash content (Table 2) support this hypothesis. For example, the ash content of SCA-700 is 41.0 wt% well below 56.0 wt% of PSC-700. As previously noted, temperatures of about 800-900 ºC are required for the chemical activation to be effective. Finally, when the activation stage is performed at 1000 ºC, the textural properties are worse than those obtained at lower temperature due to a partial degradation of the porous structure.

Consequently, from the standpoint of textural properties, the optimum activation temperature is between 800-900 ºC. These results are in good agreement with the fact reported in the literature that high temperatures are required for the physical activation with CO_2 to be effective [21,27].

3.3.2. Composition

In order to further investigate the effect of the activation process on the composition of sludge carbons, selected samples were subjected to elemental analysis and the analysis of the concentration of heavy metals. The selected samples are raw dewatered sewage sludge and the samples of sludge carbon activated at 800 ºC (SC-800, PSC-800 and SCA-800). The results are listed in Table 4.

Table 4. Results of elemental analysis and concentration of heavy metals of sewage sludge and samples activated at 800 ºC. Elemental analysis, wt%. Heavy metals, mg/kg.

Sample	C	H	N	C/H	Cr	Ni	Cu	Zn	Pd
Sewage sludge	29.7	4.1	3.2	7.2	167	586	376	3123	< 0.02
PSC-800	29.6	7.0	1.8	4.2	453	225	329	942	< 0.02
SC-800	18.0	6.3	0.9	2.9	254	140	586	5592	< 0.02
SCA-800	36.4	1.1	1.9	33.1	499	230	775	4563	< 0.02

The concentration of heavy metals in sewage sludge depends on the industrial activities around the source of sludge. Indeed, the heavy metals can be integrated in the solid fraction of the sludge and remain with the sludge during wastewater treatment processes [41].

As shown in Table 4, the effect of the activation process on the concentration of heavy metals is variable, depending on the metal. For example, the concentration of Cr increases in the sludge carbon activated at 800ºC, as compared to non -treated sample. On the contrary, the content of Ni decreases after the activation whatever the applied procedure. The concentration of Cu and Zn decreases by the acid pretreatment followed by the activation process, whereas their concentration increases through the rest of activation methods.

The increase in the concentration of some heavy metals could be interpreted as an environmental risk. However, the bioavailability and ecotoxicity of the biochars strongly depend on the specific chemical form of the heavy metals. These can be either incorporated to primary or secondary minerals, complexed with organic ligands or others. Therefore, the environmental risk is not directly related to metal concentration as reported in previous works [42,43].

The data of elemental composition in Table 4 show that the activation with CO_2 (SC-800) results in a notable decrease in carbon content, while the resulting product is enriched in inorganic fraction (C = 18 wt%, ash content =76.2 wt%). The acid pretreatment limits the mineralization of sludge carbon as deduced from its higher carbon content as compared to the only CO_2 activated sample (SC-800) and its moderate ash percentage (60.0 wt%). The C/H ratio of both PSC-800 and SC-800 decrease as compared to raw sewage sludge (C/H = 4.2 and 2.9, respectively) what reveals the loss of mainly carbonaceous material during the heat treatment. The slightly higher value measured for the acid pretreated sample suggests that the acid treatment prior to physical activation favours the occurrence of dehydrogenative polymerization and dehydrative polycondensation reactions during the activation process. These reactions are associated to significant loss of aliphatic hydrogen through olygomerization and of oxygen-containing structures through polycondensation reactions [2,44]. The FTIR results, commented in section 3.3.3., are in good agreement with this hypothesis, since it is observed an increased formation of surface functional groups for acid pretreated samples.

The acid washing after the activation with CO_2 results in an important modification of the bulk composition of the material, since the resulting char is enriched in carbon whereas the ash content is decreased due to the washing effect of the acid treatment. These results are in good agreement with the results of PSD. According to the aforementioned hypothesis, the acid washing performed after the physical activation with CO_2, once the porous structure has been developed, ensures a better accessibility of the acid to the interior of the particles, leading to a more efficient removal of the inorganic fraction, compared to the acid treatment performed prior to physical activation.

3.3.3. Surface chemistry

Figure 5 displays the FTIR spectra of all samples of sludge carbon investigated. In the case of the samples prepared by physical activation only (Fig. 7a), several small peaks are observed

between 600 and 750 cm^{-1}, attributed to the vibration of complex components of sludge carbon [22], which do not show a clear trend with the activation temperature. All samples possess a similar and predominant band at 1060 cm^{-1}, associated with the silicon content, and indicative of the presence of structures such as Si-O-Si, Si-O-X (X=Al, Fe, Ca, Mg and Na) and Si-O-C [22,45]. The small band appearing near 800 cm^{-1} could also be related to Si-O-Si structure. The peak near 1400 cm^{-1} is attributed to either $CaCO_3$ or long-chain aliphatic structures (C-H bending band) [11]. This peak is diminished as the activation temperature is increased. A prominent and well defined peak is observed for samples activated at 600 ºC, whereas at 900 ºC it is almost completely absent. This result can be explained by the accelerated decomposition of organic compounds and $CaCO_3$ at temperatures above 700 ºC. In addition, the samples prepared at temperatures between 600 and 800 ºC exhibit a shoulder close to 1600 cm^{-1} attributed to carbonyl groups (C=O) [45,46]. The height of this band diminishes with temperature and, as occurred with that near 1400 cm^{-1}, it almost disappears at temperatures above 900 ºC. The broad peak at about 3400 cm^{-1} is characteristic of –OH and –NH surface functional groups [11,18], and could be partially attributed to adsorbed water. This band is strong at 600 ºC, whereas at temperatures higher to 700 ºC it is dramatically reduced.

FIGURE 5

Figure 5b shows the results corresponding to acid washed samples. The silicon content of the materials is still evident (1060 cm^{-1}). However, there are important changes in the peaks appearing at 1400 and 1600 cm-1. The peak at 1400 cm^{-1}, a clearly resolved peak for SC samples, appears as a shoulder after acid washing. This is attributed to the removal of calcite by the acid treatment. Moreover, this shoulder decreases with temperature, revealing an increased decomposition/volatilization of aliphatic compounds. On the contrary, the band at 1600 cm^{-1} ascribed to C=O functionalities, that appears as a shoulder for SC samples, appears as a well defined peak after acid washing. This band also decreases with temperature, as occurred for SC

samples, but it is not completely depleted at 900 ºC. The effect of the acid treatment on the –OH and –NH is the same as above mentioned for C=O groups. Both functionalities increase by acid washing and decrease with temperature. Nevertheless, it is still present at high temperatures, and every sample shows a clear defined peak.

Finally, the FTIR spectra of acid pretreated samples are shown in Figure 5c. The predominant peak is that related to the silicon content of the material. The shape of the peaks at 1400 and 1600 cm^{-1} is similar to that of SCA samples. Main differences are related to C=O groups. The characteristic peak at 1600 cm^{-1} is significantly lowered by the acid pretreatment, as compared to acid washed samples. In addition, the effect of activation temperature is different. Whereas for SC and SCA samples surface C=O functionalities decrease with temperature, PSC samples show a maximum at 800 ºC. This result suggests the occurrence of two opposite effects. On the one hand, the removal of C=O functional groups as temperature increases. On the other hand, the enhancement with temperature of reaction mechanisms that involve the formation of surface functional groups. Indeed, the samples that undergo the acid pretreatment are subjected to a combined physical and chemical activation process. The broad band close to 3400 cm^{-1} shows the same trend, with a maximum at 800 ºC.

Table 2 summarizes the pH values of the prepared samples of sludge carbon. It is observed that samples obtained by physical activation only exhibit values higher than 11. Although the sludge carbons prepared by physical activation are basic in nature, our values can be deemed as high, compared to those reported in the literature [1], which could be partially explained by the heterogeneity of sewage sludge [1,30]. The acid washing leads to a decrease in the pH, which increases in all cases with the activation temperature. This effect is much more pronounced for acid pretreated samples and can be attributed to the desorption and/or decomposition of acidic functional groups [17,30,47], as confirmed by FTIR analysis (Figure 5).

3.4. Adsorption of methylene blue and phenol

Figures 6 and 7 show the adsorption isotherms of methylene blue and phenol at 20 ºC for the prepared samples of sludge carbon. Table 5 summarizes the best fitting parameters, corresponding to Redlich-Peterson model. The equations and best fitting parameters of Langmuir and Freundlich models are available as supplementary material (Tables S1 and S2).

FIGURE 6

FIGURE 7

The correlation between the experimental uptake capacity of MB and phenol (listed in Table 5) and several parameters was investigated. Table 6 summarizes the Pearson partial correlation coefficients (IBM SPSS Statistics v22). Parameters related to textural properties (S_{BET}, S_{micro}, S_{ext}, V_{micro}, V_{meso}, V_{macro}, V_{total}, D_p), sample composition and surface chemistry (ash content, amount of –OH and –NH groups, and amount of C=O groups, obtained by integrating the areas of the FTIR spectra) and adsorption performance (q_{MB}, q_{ph}) were studied.

The results show a strong and statistically significant correlation between certain textural properties and the adsorption of MB (S_{BET}, r = 0.980; S_{ext}, r = 0.925; V_{meso}, r = 902 and V_{total}, r = 0.904). The values of r were notably larger as compared to q_{ph}. The high correlation with the mesopore fraction could be expected and ascribed to the relatively large molecular size of MB [1]. Micro- and macroporosity also show a statistically significant effect, although much weaker. On the contrary, the adsorption of phenol shows a high and significant correlation with porosity in the micro range (S_{micro}, r= 0.900; V_{micro}, r = 0.904), as expected, owing to its small molecular size and the occurrence of pore wall effects.

Regarding the effect of surface chemistry, there is no relationship between the amount of –OH, -NH and C=O functional groups and the adsorption of phenol. In contrast, a clear relationship between the uptake of MB and the amount of C=O functionalities is observed.

For the samples prepared by physical activation only, the highest value of q_{exp} of both MB and phenol corresponds to SC-800 (30.2 and 13.5 mg/g, respectively). This sample possesses the highest S_{BET}, V_{micro} and V_{meso}.

Table 5. Best fit Redlich-Peterson isotherm parameters for MB and phenol adsorption and experimental uptake of both adsorbates.

	Adsorption of MB					Adsorption of phenol				
	$q_{exp,}$ mg/g	$K_{R,}$ L/g	α, $(L/mg)^{\beta}$	β	APE	q_{exp} mg/g	$K_{R,}$ L/g	α, $(L/mg)^{\beta}$	β	APE
SC-600	20.6	5.04	0.262	0.973	0.54	10.0	0.318	0.036	0.956	0.92
SC-700	16.1	5.28	0.514	0.892	2.03	8.9	0.253	0.016	1.078	4.98
SC-800	30.2	17.4	0.832	0.908	3.60	13.5	0.842	0.057	1.002	2.75
SC-900	16.5	40.6	3.609	0.909	3.72	6.5	0.283	0.069	0.897	1.18
SC-1000	5.9	0.41	0.059	0.998	0.69	3.1	0.123	0.038	0.988	1.20
Mean value					2.1					2.2
SCA-600	56.5	11.8	0.230	0.966	1.17	15.5	0.437	0.022	1.018	3.44
SCA-700	57.5	12.4	0.233	0.967	2.35	17.1	0.695	0.031	1.036	6.65
SCA-800	60.7	56.1	1.076	0.960	1.87	24.9	2.360	0.089	1.004	3.38
SCA-900	34.0	12.6	0.435	0.956	0.69	9.7	0.258	0.019	1.034	1.64
Mean value					1.5					3.8

PSC-600	8.9	0.63	0.104	0.875	1.56	6.7	0.182	0.015	1.078	3.62
PSC-700	10.0	0.62	0.083	0.883	3.12	6.5	0.192	0.040	0.919	2.01
PSC-800	32.1	18.4	0.618	0.978	0.28	23.8	0.926	0.034	1.001	0.44
PSC-900	35.0	19.9	0.998	0.869	2.10	32.4	33.2	1.784	0.900	0.68
PSC-1000	4.8	6.65	1.605	0.967	0.60	2.8	0.051	0.013	1.016	2.09
Mean value					1.5					1.8

Table 6. Pearson's partial correlation coefficients among MB and phenol uptake capacity and several parameters.

		q_{MB}	q_{ph}	S_{BET}	S_{micro}	S_{ext}	V_{micro}	V_{meso}	V_{macro}	V_{total}	D_p	-OH/-NH	C=O	Ash
q_{MB}	r	1												
	p value (two tail)													
q_{phenol}	r	0.707**	1											
	p value (two tail)	0.005												
S_{BET}	r	0.980**	0.684**	1										
	p value (two tail)	0.000	0.007											
S_{micro}	r	0.704**	0.900**	0.730**	1									
	p value (two tail)	0.005	0.000	0.003										
S_{ext}	r	0.925**	0.435	0.937**	0.445	1								
	p value (two tail)	0.000	0.120	0.000	0.111									
V_{micro}	r	0.724**	0.904**	0.750**	0.999**	0.471	1							
	p value (two tail)	0.003	0.000	0.002	0.000	0.090								
V_{meso}	r	0.902**	0.461	0.921**	0.467	0.968**	0.491	1						

	p value (two tail)	0.000	0.097	0.000	0.092	0.000	0.075						
V_{macro}	r	0.601*	0.142	0.664**	0.257	0.738**	0.272	0.740**	1				
	p value (two tail)	0.023	0.627	0.010	0.374	0.003	0.346	0.002					
V_{total}	r	0.904**	0.489	0.938**	0.537*	0.954**	0.558*	0.980**	0.835**	1			
	p value (two tail)	0.000	0.076	0.000	0.048	0.000	0.038	0.000	0.000				
D_p	r	-0.146	-0.329	-0.192	-0.459	-0.016	-0.457	0.109	0.342	0.109	1		
	p value (two tail)	0.619	0.250	0.512	0.099	0.956	0.101	0.711	0.231	0.712			
-OH/-NH	r	0.319	0.031	0.262	0.109	0.287	0.114	0.224	0.436	0.294	0.176	1	
	p value (two tail)	0.266	0.915	0.366	0.711	0.320	0.698	0.441	0.119	0.308	0.548		
C=O	r	0.675**	0.349	0.577*	0.295	0.606*	0.314	0.541*	0.328	0.518	0.065	0.633	1
	p value (two tail)	0.008	0.221	0.031	0.306	0.022	0.274	0.046	0.252	0.058	0.825	0.015	
Ash	r	-0.664**	-0.402	-0.613	-0.358	-0.621*	-0.376	-0.598*	-0.547*	-0.626*	-0.210	-0.581*	-0.900*
	p value (two tail)	0.010	0.154	0.020	0.208	0.018	0.185	0.024	0.043	0.017	0.471	0.029	0.000

Experimental points = 14

** Correlation significant at the 99 % level of confidence

* Correlation significant at the 95 % level of confidence

Among the materials subjected to acid washing, the maximum removal ability of MB (60.7 mg/g) and phenol (24.9 mg/g) is obtained using SCA-800. For both adsorbates, the acid washing increases two-fold the equilibrium uptake capacity. The maximum uptake capacity of phenol can be explained by the value of S_{micro} and S_{BET} of SCA-800, the highest of SCA samples.

Concerning the uptake of MB, SCA-800 provides the highest value of all samples. Nevertheless, slight difference is obtained for SCA-600 and SCA-700 (56.5 and 57.5 mg/g, respectively). As the activation temperature increases from 600 to 800 ºC, there is an increase in S_{BET} (from 260 to 339 m^2/g) and V_{meso} (from 0.1907 to 0.3255 cm^3/g). However, there is also a decrease in carbonyl groups (Figure 5b). It is known that oxygen-containing functional groups represent electron-rich surface sites, which favour the adsorption of basic solutes, such as cationic MB. The occurrence of these counter effects, would explain the little variation in the values of q_{exp} in the 600-800 ºC range. On the other hand, the relatively low q_{exp} of SCA-900 (34.0 mg/g) is noteworthy, compared to the samples prepared using lower activation temperature. This low uptake capacity could be related to surface chemistry. Indeed, SCA-900 shows a very low amount of carbonyl groups, much lower than that of SCA-600, SCA-700 and SCA-800 (band at 1600 cm^{-1} in Figure 5b).

The post-washing step favours the adsorption of methylene blue to a greater extent than that of phenol. In fact, the uptake capacity of SCA-600 is almost three times higher than that of SC-600 (56.5 vs 20.6 mg/g), and twice as much as the maximum value obtained using physical activation only. Consequently, the utilization of a moderate activation temperature (600 ºC) combined with the acid washing, results in a material with a high MB removal ability.

Among the acid pretreated samples, the maximum uptake capacity of both MB and phenol (35.0 mg/g and 32.4 mg/g, respectively) is obtained upon activation at 900 ºC (PSC-900). In the case

of MB, this adsorption capacity is only slightly higher than the maximum value achieved through physical activation only (30.2 mg/g). The q_{exp} of MB of PSC-800 is also noteworthy, which is only slightly lower (32.1 mg/g), whereas there is a large difference between the V_{meso} of both samples (0.0286 vs 0.0758 cm^3/g). Again, the relevance of a suitable surface chemistry becomes evident, as the higher amount of C=O functionalities of PSC-800 (Figure 5c) could compensate for less suitable textural properties.

In contrast, the pre-washing step results in a great improvement in the phenol removal ability (an increase of 140 % of PSC-900, compared to the maximum value obtained through physical activation only). Regarding the adsorption of phenol, it is noteworthy that PSC-800 and PSC-900 possess a different uptake capacity, whereas both samples have a similar microporosity (S_{micro} is 112 and 109 m^2/g, respectively). This result shows the implication of other factors in the adsorption process. In fact, it has been proposed in the literature that phenol could be adsorbed not only by physisorption, but also by surface polymerization [48]. The presence of metals on the surface of the material would favour this mechanism. The higher amount of ash of PSC-900, compared to PSC-800 (77.7 vs. 60.0 wt%) could then favour its phenol adsorption capacity. However, no statistical evidence is observed from the Pearson correlation coefficients calculated for the ash content (Table 6).

Table 7 summarizes the methylene blue and phenol adsorption capacity of various materials, prepared from sewage sludge. Although the adsorbents were prepared using different experimental conditions, the results are useful for comparison purposes. It is observed that the maximum uptake capacity obtained in this study can be considered as medium to high. The materials that possess higher adsorption capacity were prepared either by chemical activation with $ZnCl_2$ followed by acid washing, or by physical activation with steam. Moreover, in the case of methylene blue, the material prepared by physical activation with steam was prepared using paper mill sewage sludge as a precursor.

Table 7. MB and phenol uptake capacity of various adsorbents prepared from sewage sludge.

Sludge type	Preparation conditions	Adsorbate	Uptake (mg/g)	Reference
Sludge from an urban WWTP	Carbonization: 700 ºC, 300 min.	MB	12	[49]
Sludge from an urban WWTP	Carbonization: 650 ºC, 30 min.	MB	17	[50]
Paper mill sewage sludge	Carbonization: 300 ºC, 60 min.	MB	25	[15]
Paper mill sewage sludge	Carbonization: 800 ºC, 360 min.	MB	35	[51]
Sludge from an urban WWTP	Phys. act.: CO_2, 800 ºC, 30 min. Post-treatment: acid washing (HCl).	MB	61	This study
Sludge from an urban WWTP	Chem. act.: $ZnCl_2$, 650 ºC, 120 min. Post-treatment: acid washing (HCl).	MB	91	[46]
Paper mill sewage sludge	Carbonization: 300 ºC, 60 min. Phys. act.: H_2O, 850 ºC, 40 min.	MB	130	[15]
Sludge from an urban WWTP	Chem. act.: KOH, 600 ºC, 60 min. Post-treatment: acid washing (HCl)	Phenol	18	[52]
Sludge from an urban WWTP	Carbonization: 650 ºC, 30 min.	Phenol	25	[50]
Sludge from an urban WWTP	Chem. act.: H_2SO_4, 650 ºC, 30 min. Post-treatment: acid washing (HCl).	Phenol	25	[50]
Sludge from an urban WWTP	Chem. act.: H_2SO_4, 650 ºC, 60 min.	Phenol	26	[53]
Sludge from an urban WWTP	Pre-treatment: acid washing (HCl). Phys. act.: CO_2, 900 ºC, 30 min.	Phenol	32	This study

Sludge from an urban WWTP	Carbonization: 600 ºC, 60 min. Phys. act.: H_2O, 760 ºC, 30 min.	Phenol	44	[14]
Sludge from an urban WWTP	Chem. act.: $ZnCl_2$, 650 ºC, 5 min. Post-treatment: acid washing (HCl).	Phenol	82	[50]

4. Conclusions

This study investigated the physical activation of sewage sludge with CO_2. The findings reveal that the following reactions and processes take place: (i) the reaction of CO_2 with carbon; (ii) the decomposition/volatilization of organic matter; (iii) the decomposition/volatilization of inorganic compounds (such as calcium carbonate); (iv) the desorption of water and (v) the reaction of the OH- functionalities with carbon to form products such as HCN. All these reactions involve the release of gaseous compounds and thus, are expected to generate porosity.

From the standpoint of textural properties, the optimum activation temperature is 800 ºC for untreated (SC) and acid washed (SCA) samples, and 800-900 ºC for acid pretreated samples (PSC). The acid treatment (either before or after physical activation) significantly increases the porosity in the whole pore size range, the increase in micropores being noteworthy. The post-washing increases the porosity to a greater extent, mainly through a pore unblocking mechanism.

The results show that the post-washing increases the amount of surface C=O, –OH and –NH functionalities. These functionalities decrease with temperature for SC and SCA samples. When the acid pretreatment is performed, textural properties are maximized at 800 ºC, attributed to two opposite effects of temperature: the depletion of functional groups, and the enhancement of reactions involving HCl.

There is a significant and positive correlation between the textural properties (mainly S_{BET}, V_{total} and V_{meso}), surface chemistry (amount of carbonyl groups) and the uptake of MB. SCA-800 has the highest MB removal ability (60.7 mg/g), whereas the good performance of SCA-600 (56.5 mg/g) should be highlighted, since the moderate activation temperature used results in a reduction of the preparation cost. The adsorption of phenol is favoured by sludge carbons with a

high degree of microporosity (S_{BET} has also influence, to a lesser extent), with no significant effect of surface functionalities. PSC-900 provides the highest phenol removal ability (32.4 mg/g).

Acknowledgements

The authors wish to thank the Basque Government (UFI 11/39 (UPV/EHU) and S-PE13UN100 project) for their economic support. The authors are also grateful for the technical and human support provided by SCAB and SCAA (SGIker) of UPV/EHU and European funding (ERDF and ESF).

References

[1] K.M. Smith, G.D. Fowler, S. Pullket, N.J.D. Graham, Water Res. 43 (2009) 2569-2594.

[2] M.J. Martin, A. Artola, M.D. Balaguer, M. Rigola, Chem. Eng. J. 94 (2003) 231-239.

[3] M. Otero, F. Rozada, L.F. Calvo, A.I. García, A. Morán, Dyes and Pigments. 57 (2003) 55-65.

[4] X. Xi, X. Guo, Journal of Molecular Liquids. 183 (2013) 26-30.

[5] X. Wang, X. Liang, Y. Wang, X. Wang, M. Liu, D. Yin, S. Xia, J. Zhao, Y. Zhang, Desalination. 278 (2011) 231-237.

[6] M. Hunsom, C. Autthanit, Chem. Eng. J. 229 (2013) 334-343.

[7] T. Boualem, A. Debab, A. Martínez de Yuso, M.T. Izquierdo, J. Environ. Manage. 140 (2014) 145-151.

[8] M.A. Lillo-Ródenas, A. Ros, E. Fuente, M.A. Montes-Morán, M.J. Martin, A. Linares-Solano, Chem. Eng. J. 142 (2008) 168-174.

[9] J.M. de Andrés, L. Orjales, A. Narros, de la Fuente, María,del Mar, M.E. Rodríguez, J. Air Waste Manage. Assoc. 63 (2013) 557-564.

[10] Y. Li, Y. Li, L. Li, X. Shi, Z. Wang, Advanced Powder Technology. 27 (2016) 684-691.

[11] A. Ros, M.A. Lillo-Ródenas, E. Fuente, M.A. Montes-Morán, M.J. Martín, A. Linares-Solano, Chemosphere. 65 (2006) 132-140.

[12] A. Gupta, A. Garg, Bioresour. Technol. 194 (2015) 214-224.

[13] R.R.N. Marques, F. Stüber, K.M. Smith, A. Fabregat, C. Bengoa, J. Font, A. Fortuny, S. Pullket, G.D. Fowler, N.J.D. Graham, Applied Catalysis B: Environmental. 101 (2011) 306-316.

[14] S. Rio, L. Le Coq, C. Faur, D. Lecomte, P. Le Cloirec, Process Saf. Environ. Prot. 84 (2006) 258-264.

[15] W. Li, Q. Yue, B. Gao, X. Wang, Y. Qi, Y. Zhao, Y. Li, Desalination. 278 (2011) 179-185.

[16] I. Velghe, R. Carleer, J. Yperman, S. Schreurs, J. D'Haen, Water Res. 46 (2012) 2783-2794.

[17] A. Méndez, G. Gascó, M.M.A. Freitas, G. Siebielec, T. Stuczynski, J.L. Figueiredo, Chem. Eng. J. 108 (2005) 169-177.

[18] C. Jindarom, V. Meeyoo, B. Kitiyanan, T. Rirksomboon, P. Rangsunvigit, Chem. Eng. J. 133 (2007) 239-246.

[19] V.M. Monsalvo, A.F. Mohedano, J.J. Rodriguez, Desalination. 277 (2011) 377-382.

[20] I. Sierra, U. Iriarte-Velasco, E.A. Cepeda, M. Gamero, A.T. Aguayo, Desalination and Water Treatment. (2015) 1-13.

[21] G. Xu, X. Yang, L. Spinosa, J. Environ. Manage. 151 (2015) 221-232.

[22] J. Zou, Y. Dai, X. Wang, Z. Ren, C. Tian, K. Pan, S. Li, M. Abuobeidah, H. Fu, Bioresour. Technol. 142 (2013) 209-217.

[23] F. Rodríguez-Reinoso, M. Molina-Sabio, M.T. González, Carbon. 33 (1995) 15-23.

[24] A. Bagreev, S. Bashkova, D.C. Locke, T.J. Bandosz, Environ. Sci. Technol. 35 (2001) 1537-1543.

[25] J.D. González, M.R. Kim, E.L. Buonomo, P.R. Bonelli, A.L. Cukierman, Energy Sources, Part A: Recovery, Utilization, and Environmental Effects. 30 (2008) 809-817.

[26] J. Donald, Y. Ohtsuka, C.(. Xu, Mater Lett. 65 (2011) 744-747.

[27] P. Hadi, M. Xu, C. Ning, C. Sze Ki Lin, G. McKay, Chem. Eng. J. 260 (2015) 895-906.

[28] C.H. Tessmer, R.D. Vidic, L.J. Uranowski, Environ. Sci. Technol. 31 (1997) 1872-1878.

[29] R. Font, A. Fullana, J.A. Conesa, F. Llavador, J. Anal. Appl. Pyrolysis. 58–59 (2001) 927-941.

[30] G. Gascó, C.G. Blanco, F. Guerrero, A.M. Méndez Lázaro, J. Anal. Appl. Pyrolysis. 74 (2005) 413-420.

[31] M. Otero, L.F. Calvo, B. Estrada, A.I. García, A. Morán, Thermochimica Acta. 389 (2002) 121-132.

[32] W. Zuo, B. Jin, Y. Huang, Y. Sun, Journal of Thermal Analysis and Calorimetry. 121 (2015) 1297-1307.

[33] L. Nowicki, S. Ledakowicz, J. Anal. Appl. Pyrolysis. 110 (2014) 220-228.

[34] U. Iriarte-Velasco, J.L. Ayastuy, L. Zudaire, I. Sierra, Chem. Eng. J. 251 (2014) 217-227.

[35] J.A. Conesa, A. Marcilla, R. Moral, J. Moreno-Caselles, A. Perez-Espinosa, Thermochimica Acta. 313 (1998) 63-73.

[36] W. Xiaohua, J. Jiancheng, Energy Procedia. 14 (2012) 1648-1652.

[37] Y. Qi, Q. Yue, S. Han, M. Yue, B. Gao, H. Yu, T. Shao, J. Hazard. Mater. 176 (2010) 76-84.

[38] A. Robau-Sánchez, A. Aguilar-Elguézabal, J. Aguilar-Pliego, Microporous and Mesoporous Materials. 85 (2005) 331-339.

[39] J.A. Caballero, R. Front, A. Marcilla, J.A. Conesa, J. Anal. Appl. Pyrolysis. 40–41 (1997) 433-450.

[40] K. Mahapatra, D.S. Ramteke, L.J. Paliwal, J. Anal. Appl. Pyrolysis. 95 (2012) 79-86.

[41] J. Werther, T. Ogada, Progress in Energy and Combustion Science. 25 (1999) 55-116.

[42] X. Yuan, H. Huang, G. Zeng, H. Li, J. Wang, C. Zhou, H. Zhu, X. Pei, Z. Liu, Z. Liu, Bioresour. Technol. 102 (2011) 4104-4110.

[43] L. Leng, X. Yuan, H. Huang, H. Jiang, X. Chen, G. Zeng, Bioresour. Technol. 167 (2014) 144-150.

[44] L. Leng, X. Yuan, H. Huang, J. Shao, H. Wang, X. Chen, G. Zeng, Appl. Surf. Sci. 346 (2015) 223-231.

[45] K.M. Smith, G.D. Fowler, S. Pullket, N.J.D. Graham, Separation and Purification Technology. 98 (2012) 240-248.

[46] L. Shi, G. Zhang, D. Wei, T. Yan, X. Xue, S. Shi, Q. Wei, Journal of Molecular Liquids. 198 (2014) 334-340.

[47] M. Hofman, R. Pietrzak, Chem. Eng. J. 183 (2012) 278-283.

[48] C.-. Leng, N.G. Pinto, Carbon. 35 (1997) 1375-1385.

[49] H. Djati Utomo, X.C. Ong, S.M.S. Lim, G.C.B. Ong, P. Li, Int. Biodeterior. Biodegrad. 85 (2013) 460-465.

[50] F. Rozada, M. Otero, J.B. Parra, A. Morán, A.I. García, Chem. Eng. J. 114 (2005) 161-169.

[51] M. Hojamberdiev, Y. Kameshima, A. Nakajima, K. Okada, Z. Kadirova, J. Hazard. Mater. 151 (2008) 710-719.

[52] A. Gupta, A. Garg, Clean Technologies and Environmental Policy. 17 (2015) 1619-1631.

[53] S. Bousba, A.H. Meniai, Chemical Engineering Transactions. 40 (2014) 235-240.

Figure captions

Figure 1. Thermal behaviour of sewage sludge under inert and oxidizing atmospheres.

Figure 2. MS curves of the main components under (a) inert atmosphere (b) oxidizing atmosphere.

Figure 3. Pore size distribution of sludge carbons activated at different temperatures. a) Samples prepared by physical activation with CO_2; b) acid washed samples and c) acid pretreated samples.

Figure 4. Evolution of corrected BET surface area with temperature for SC, SCA and PSC samples.

Figure 5. FTIR spectra of samples of sludge carbon, prepared using different activation temperatures. a) Samples prepared by physical activation with CO2; b) acid washed samples; c) acid pretreated samples.

Figure 6. Isotherm data for MB adsorption at 20 ºC by sludge carbons prepared using different activation temperatures. a) Samples prepared by physical activation with CO_2; b) acid washed samples and c) acid pretreated samples. Lines represent Redlich-Peterson model prediction.

Figure 7. Isotherm data for phenol adsorption at 20 ºC by sludge carbons prepared using different activation temperatures. a) Samples prepared by physical activation with CO_2; b) acid washed samples and c) acid pretreated samples. Lines represent Redlich-Peterson model prediction.

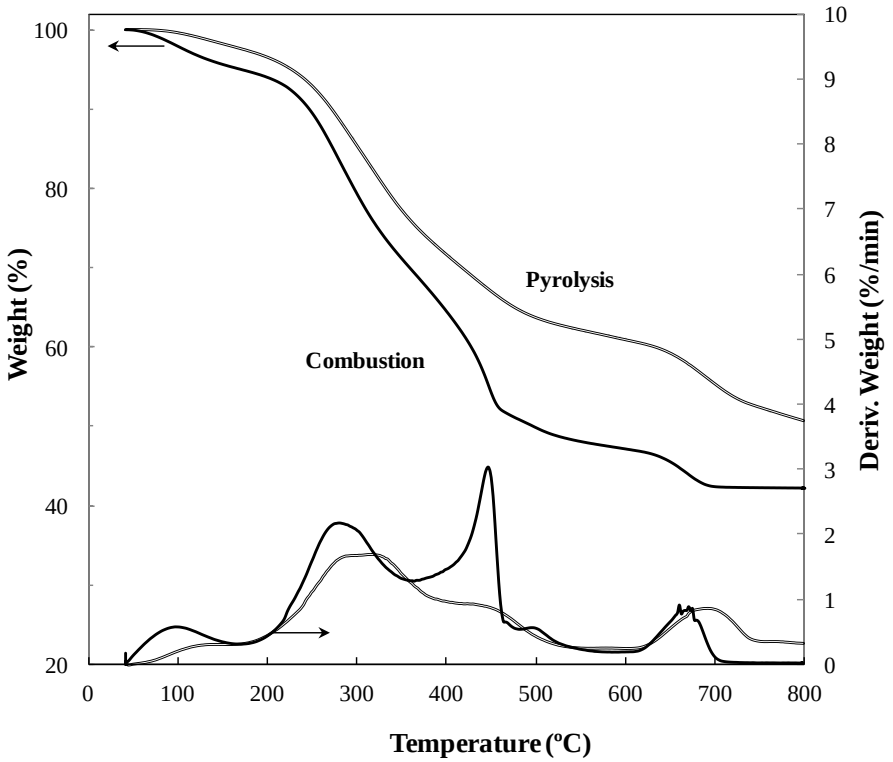
Weight (%)
Deriv. Weight (%/min)
Temperature (°C)
Pyrolysis
Combustion
100
80
60
40
20
10
9
8
7
6
5
4
3
2
1
0
0
100
200
300
400
500
600
700
800

Fig. 1

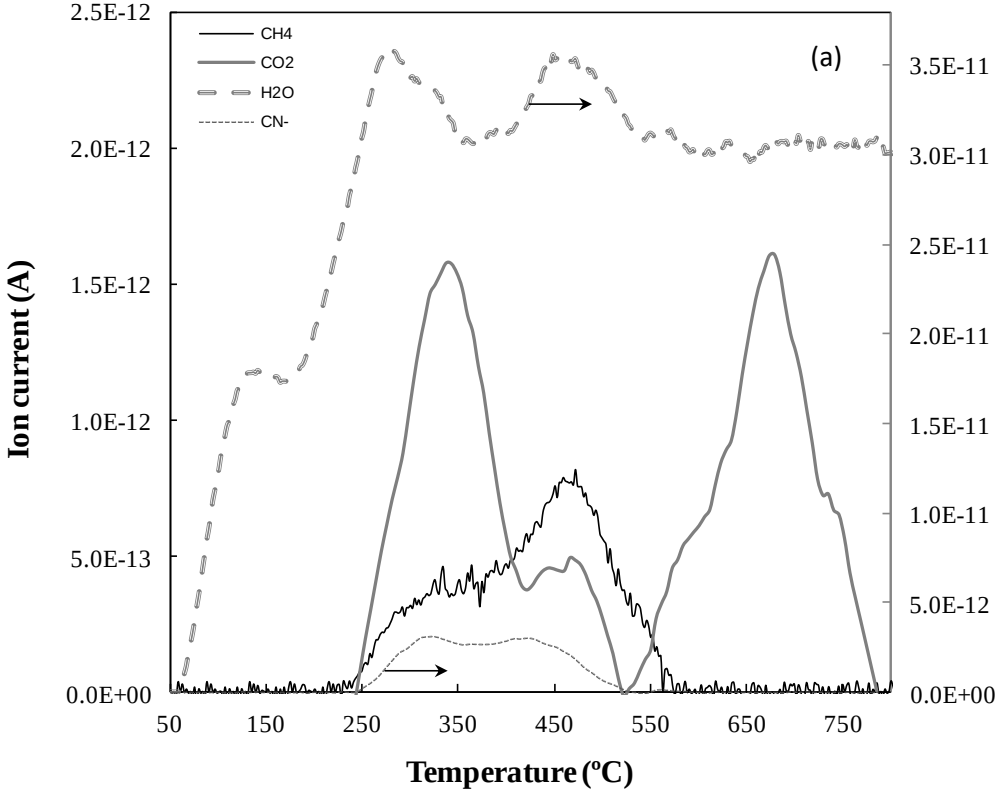
(a)
CH4
CO2
H2O
CN-
Ion current (A)
Temperature (ºC)
2.5E-12
2.0E-12
1.5E-12
1.0E-12
5.0E-13
0.0E+00
3.5E-11
3.0E-11
2.5E-11
2.0E-11
1.5E-11
1.0E-11
5.0E-12
0.0E+00
50
150
250
350
450
550
650
750

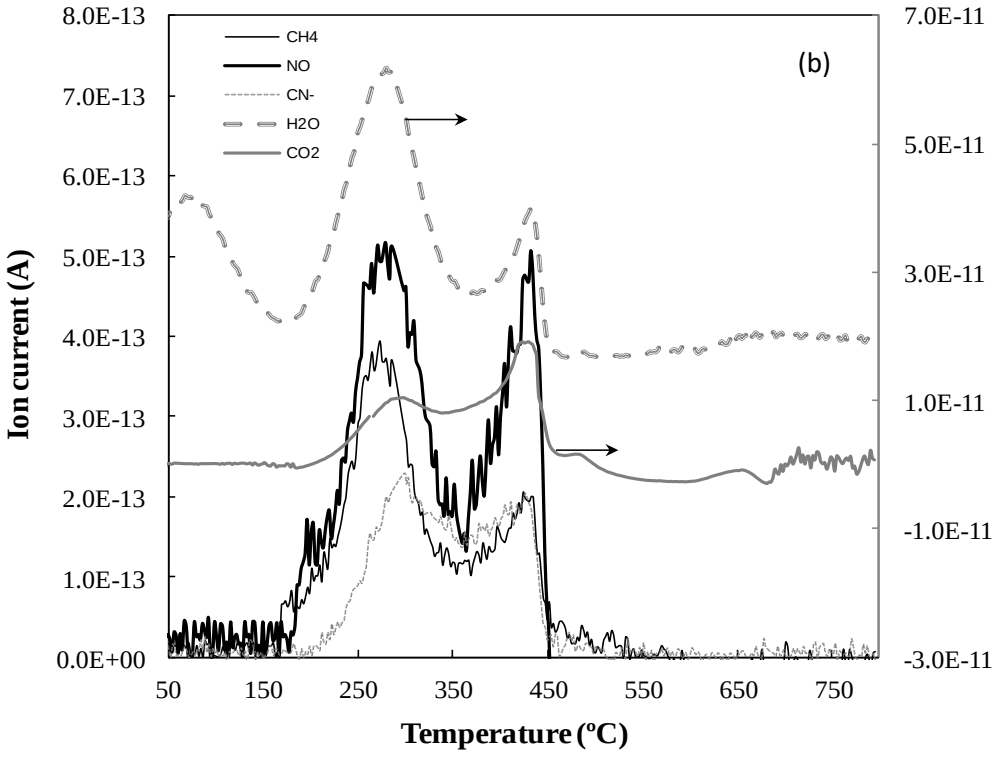
(b)
CH4
NO
CN-
H2O
CO2
Ion current (A)
Temperature (ºC)
8.0E-13
7.0E-13
6.0E-13
5.0E-13
4.0E-13
3.0E-13
2.0E-13
1.0E-13
0.0E+00
7.0E-11
5.0E-11
3.0E-11
1.0E-11
-1.0E-11
-3.0E-11
50
150
250
350
450
550
650
750

Fig. 2

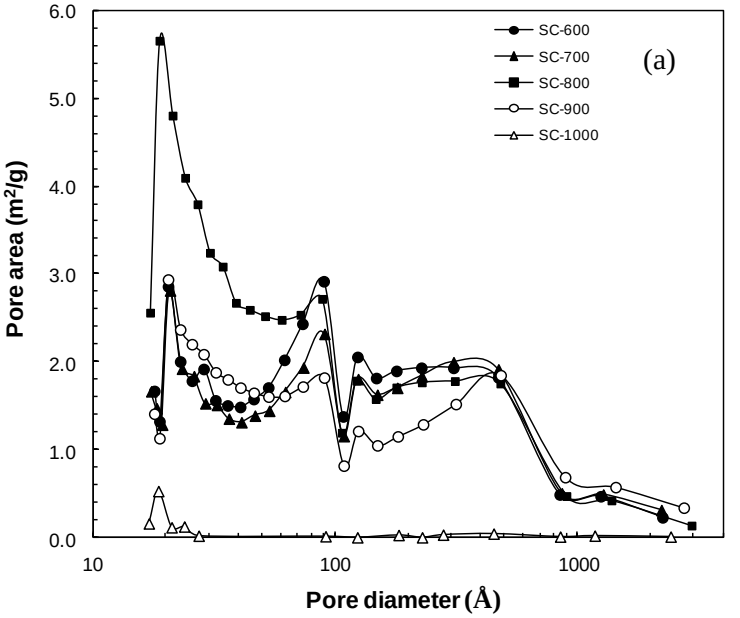
SC-600
SC-700
SC-800
SC-900
SC-1000
(a)
Pore area (m²/g)
Pore diameter (Å)

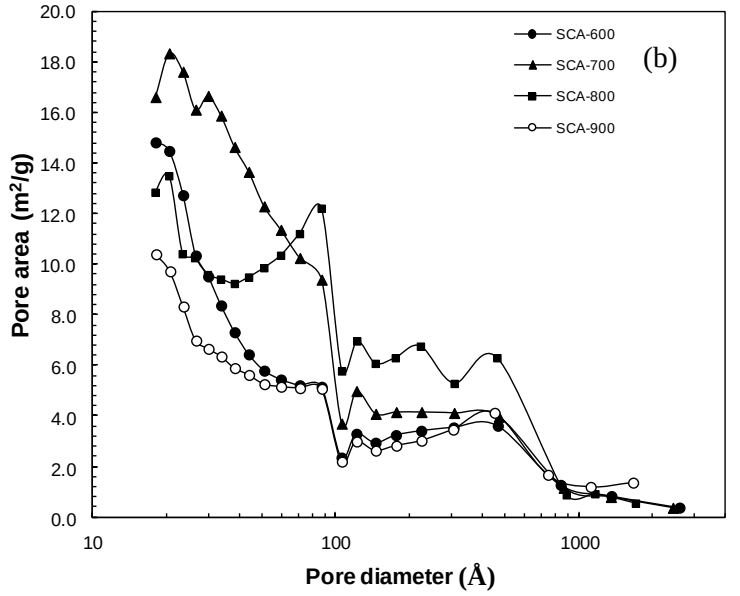
SCA-600
SCA-700
SCA-800
SCA-900
(b)
Pore area (m²/g)
Pore diameter (Å)

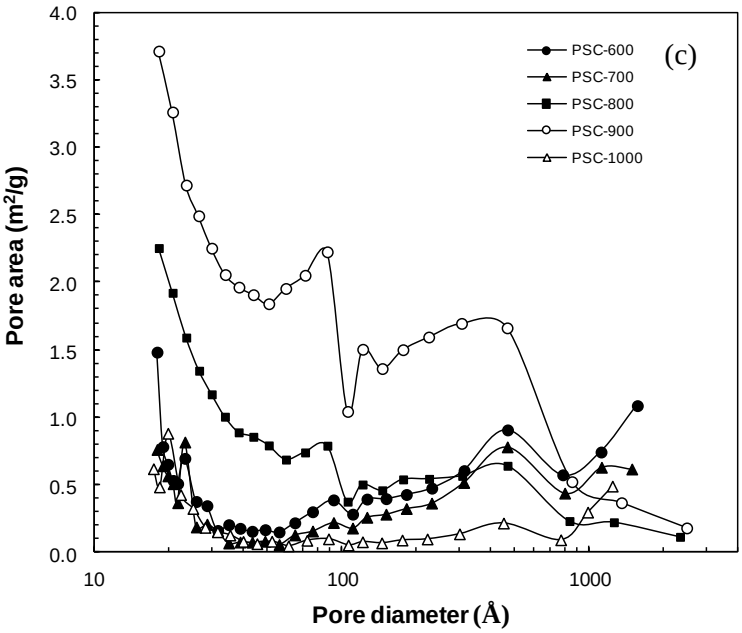
PSC-600
PSC-700
PSC-800
PSC-900
PSC-1000
(c)
Pore area (m²/g)
Pore diameter (Å)

Fig. 3

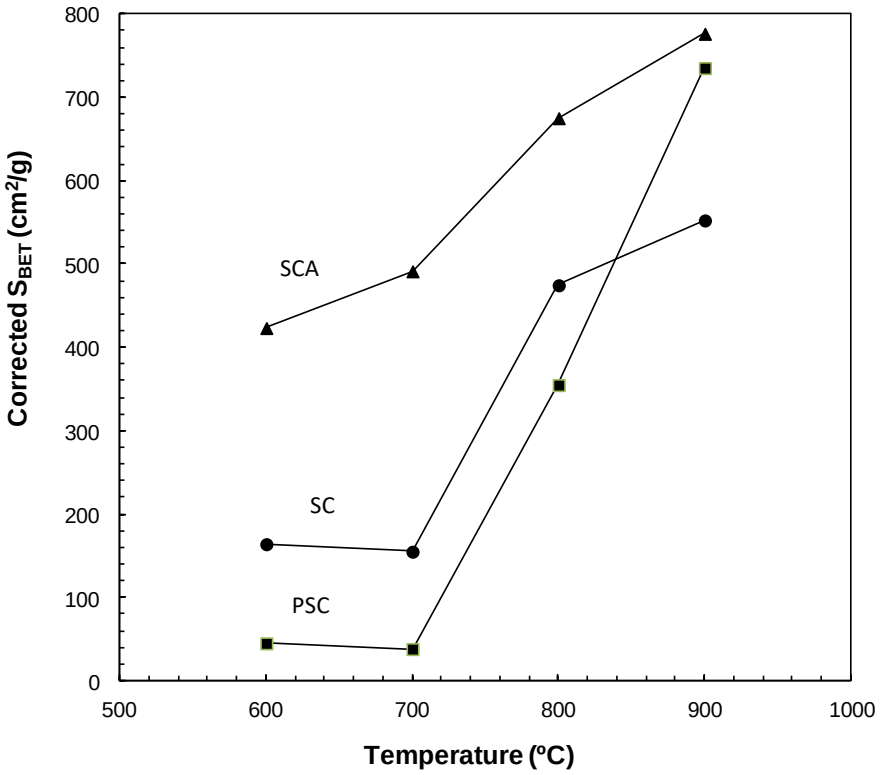
800
700
600
500
400
300
200
100
0
500
600
700
800
900
1000
Corrected S_{BET} (cm^2/g)
Temperature (ºC)
SCA
SC
PSC

Fig. 4

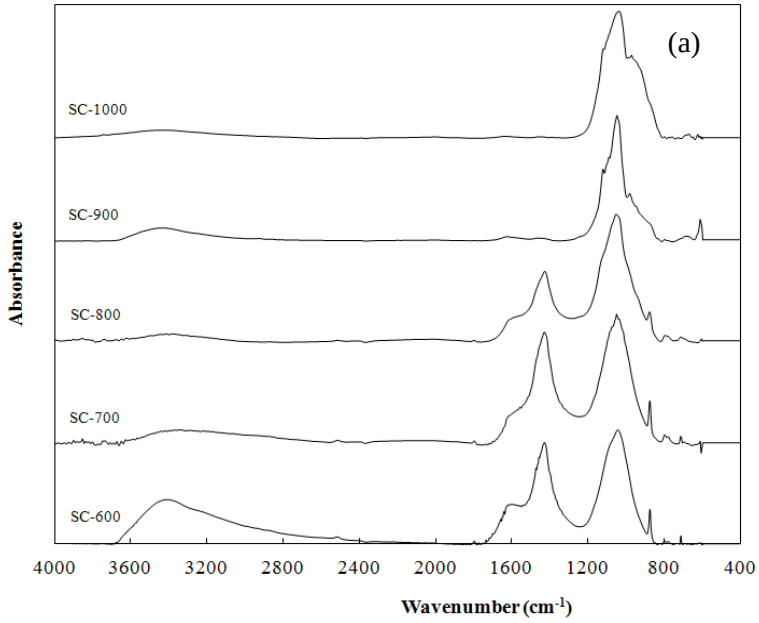
(a)
SC-1000
SC-900
SC-800
SC-700
SC-600
Absorbance
4000 3600 3200 2800 2400 2000 1600 1200 800 400
Wavenumber (cm-1)

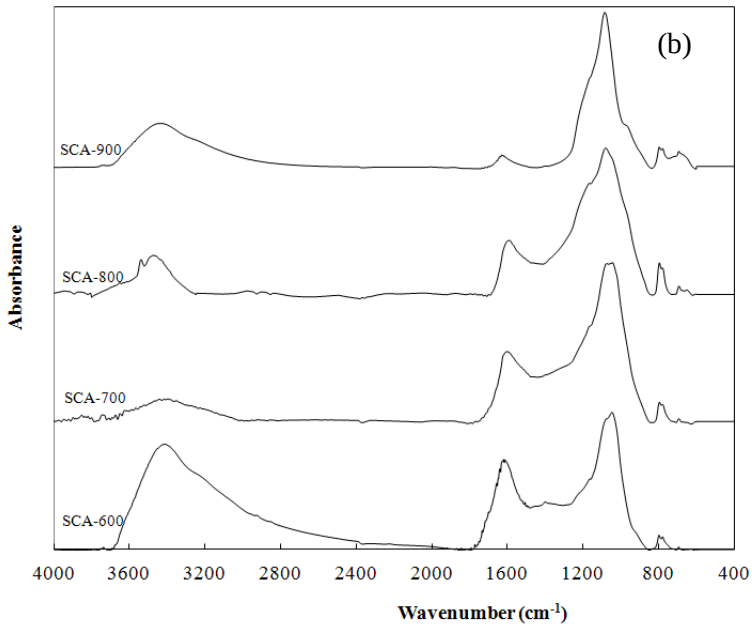
(b)
SCA-900
SCA-800
SCA-700
SCA-600
Absorbance
4000 3600 3200 2800 2400 2000 1600 1200 800 400
Wavenumber (cm-1)

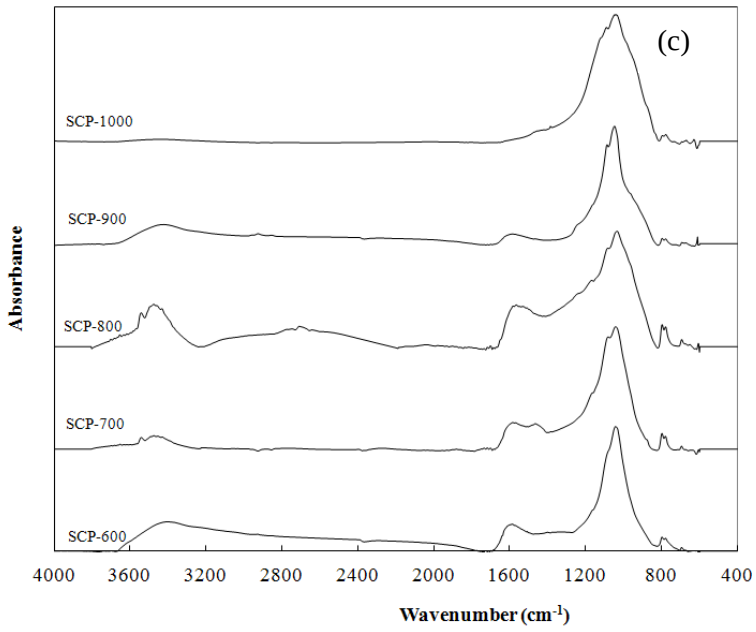
(c)
SCP-1000
SCP-900
SCP-800
SCP-700
SCP-600
Absorbance
4000 3600 3200 2800 2400 2000 1600 1200 800 400
Wavenumber (cm-1)

Fig. 5

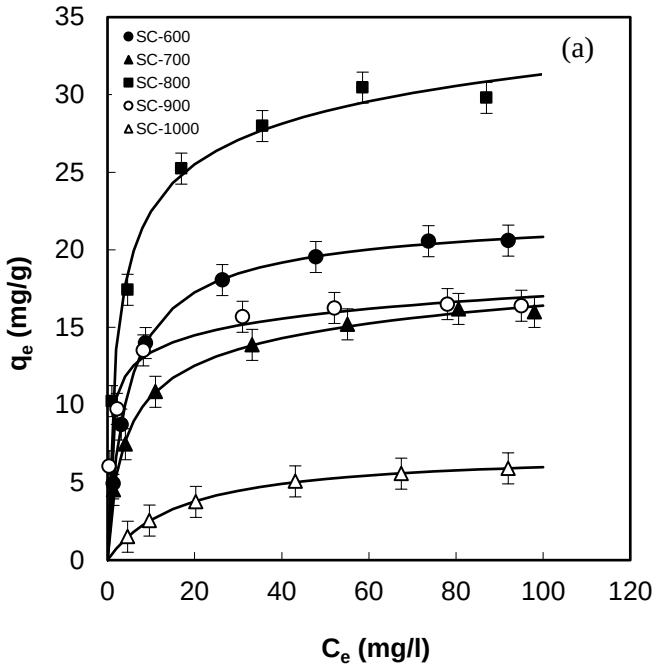
(a)
SC-600
SC-700
SC-800
SC-900
SC-1000
q_e (mg/g)
C_e (mg/l)

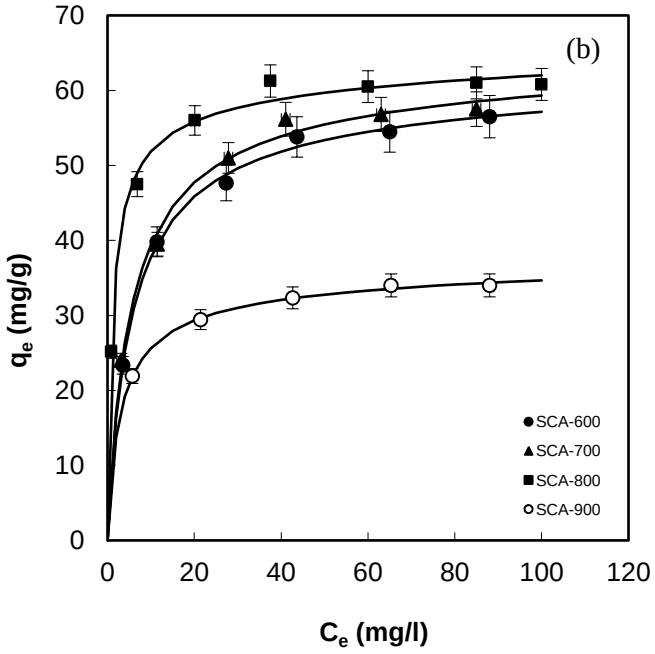
(b)
SCA-600
SCA-700
SCA-800
SCA-900
q_e (mg/g)
C_e (mg/l)

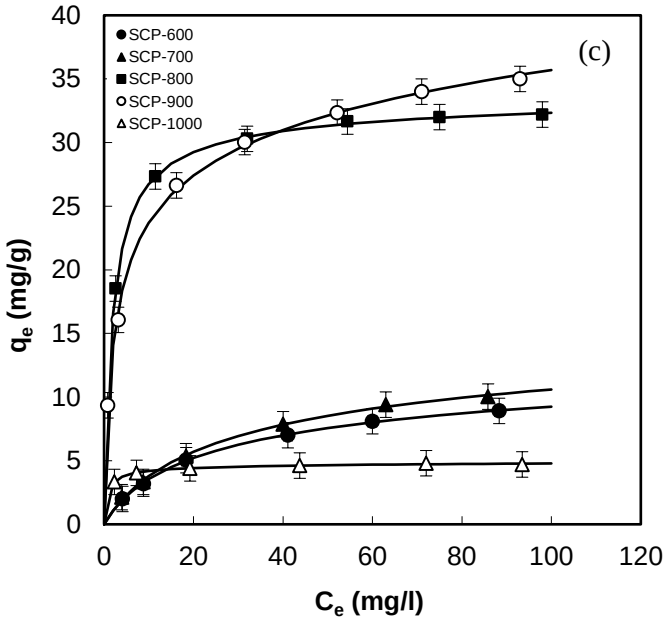
(c)
SCP-600
SCP-700
SCP-800
SCP-900
SCP-1000
q_e (mg/g)
C_e (mg/l)

Fig. 6

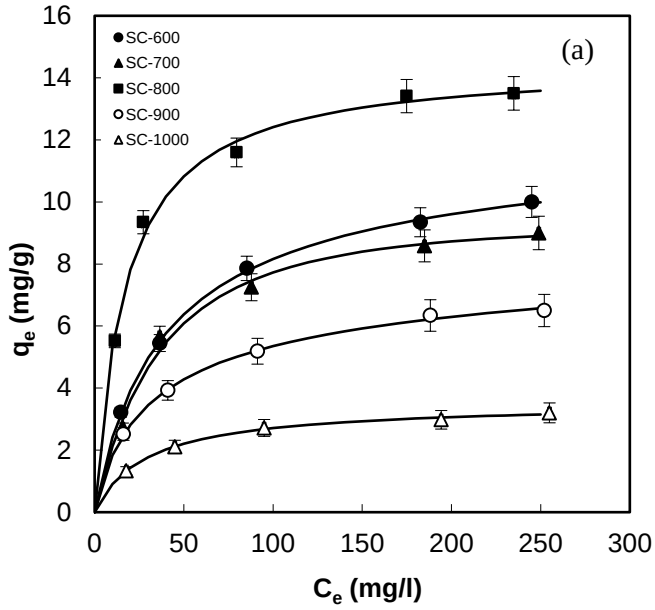
(a)
SC-600
SC-700
SC-800
SC-900
SC-1000
q_e (mg/g)
C_e (mg/l)
0
2
4
6
8
10
12
14
16
0
50
100
150
200
250
300

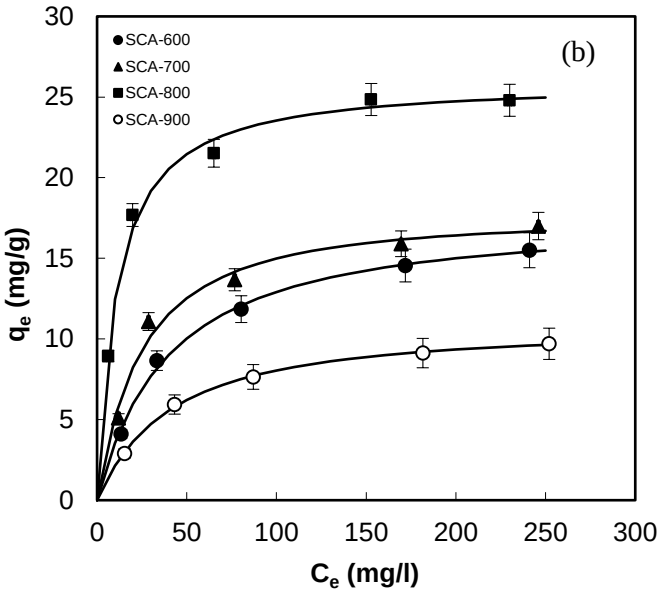
(b)
SCA-600
SCA-700
SCA-800
SCA-900
q_e (mg/g)
C_e (mg/l)
0
5
10
15
20
25
30
0
50
100
150
200
250
300

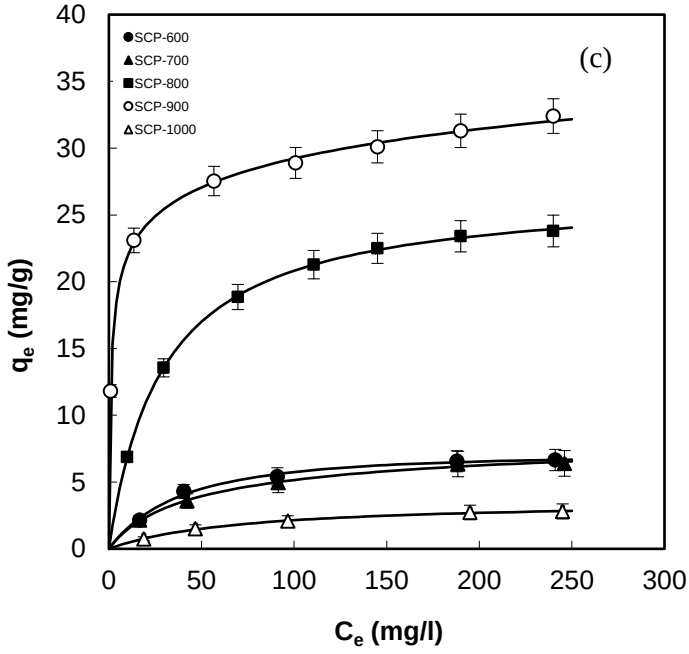
(c)
SCP-600
SCP-700
SCP-800
SCP-900
SCP-1000
q_e (mg/g)
C_e (mg/l)
0
5
10
15
20
25
30
35
40
0
50
100
150
200
250
300

Fig. 7